

# Towards an assessment of the accuracy of density functional theory for first principles simulations of water II

Eric Schwegler, Jeffrey C. Grossman, Francois Gygi, and Giulia Galli  
Lawrence Livermore National Laboratory, P.O. Box 808, Livermore, California 94559  
(dated: January 12, 2022)

A series of 20 ps ab initio molecular dynamics simulations of water at ambient density and temperatures ranging from 300 to 450 K are presented. Car-Parrinello (CP) and Born-Oppenheimer (BO) molecular dynamics techniques are compared for systems containing 54 and 64 water molecules. At 300 K, excellent agreement is found between radial distribution functions (RDFs) obtained with BO and CP dynamics, provided an appropriately small value of the fictitious mass parameter is used in the CP simulation. However, we find that the diffusion coefficients computed from CP dynamics are approximately two times larger than those obtained with BO simulations for  $T > 400$  K, where statistically meaningful comparisons can be made. Overall, both BO and CP dynamics at 300 K yield overstructured RDFs and slow diffusion as compared to experiment. In order to understand these discrepancies, the effect of proton quantum motion is investigated with the use of empirical interaction potentials. We find that proton quantum effects may have a larger impact than previously thought on structure and diffusion of the liquid.

## I. INTRODUCTION

Recently, a number of studies have focused on understanding in detail the level of accuracy that can be achieved in ab initio molecular dynamics simulations of water<sup>1,2,3</sup>. In particular, it was found in both Ref.<sup>2</sup> and<sup>3</sup> that in the absence of proton quantum effects, density functional theory (DFT) within widely used generalized gradient approximations (PBE<sup>4</sup> and BLYP<sup>5,6</sup>) leads to significantly overstructured radial distribution functions (RDFs) and slower diffusion than experiment, at ambient temperature and pressure.

In our previous work<sup>3</sup>, within the Car-Parrinello (CP) method<sup>7</sup>, we found that using either the Perdew-Burke-Ernzerhof (PBE)<sup>4</sup> or the Becke-Lee-Yang-Parr (BLYP)<sup>5,6</sup> functional leads to very small differences in the structural properties of the room temperature liquid. Size effects, although not fully negligible when using 32 molecule cells, were found to be rather small. We also found that there is a wide range of ratios ( $\approx M$ ) between the fictitious electronic mass ( $m_f$ ) and the smallest ionic mass of the system (either  $M_H = 1836$  au for hydrogen or  $M_D = 3672$  au for deuterium atoms) for which the electronic ground state is accurately described in micro-canonical CP simulations ( $\approx M = 1/5$ ). However, care must be exercised not to carry out simulations outside this range, where structural properties may artificially depend on  $m_f$ . Specifically, our results showed that the use of  $\approx M = 1/3$  leads to an artificial softening of the pair correlation functions, which are in fortuitous agreement with experiment. In the case of an accurate description of the electronic ground state, and in the absence of proton quantum effects, the oxygen-oxygen RDF is found to be over-structured compared with that obtained in neutron scattering<sup>8</sup> and x-ray diffraction experiments<sup>9</sup> and the computed diffusion coefficients are 10 to 20 times smaller than experiment. In our previous work<sup>3</sup>, we also examined the amount of sampling needed to obtain statistically independent data points for calculated proper-

ties, and showed that for segments of the oxygen-oxygen RDF the data correlation time is quite long; time intervals as large as 10-20 ps are required to obtain a single statistically independent data point (correlation time is not to be confused with equilibration time, as we will discuss later in the text.)

Although a number of important technical parameters were tested in Ref.<sup>3</sup>, several questions remain unanswered. First, it is important to fully test the convergence of the CP algorithm as the value of the fictitious mass approaches zero and to investigate whether possible sources of inaccuracies, such as those pointed out by Tangney and Scandolo<sup>10</sup> persist even for small  $\approx M$  ratios ( $\approx M = 1/5$ ). In order to address this issue, we present here a series of ab initio MD simulations at different temperatures, using both the CP method and minimizing the Kohn-Sham energy functional at each MD time step, while keeping all the other parameters of the two calculations fixed. We refer to this direct minimization technique as Born-Oppenheimer (BO) MD. Our results show an excellent agreement between RDFs obtained in CP and BO simulations, provided an appropriately small value of the fictitious electronic mass is used ( $\approx M = 1/5$ ), in agreement with previous BO simulations<sup>2</sup>. However, diffusion coefficients obtained within BO and CP simulations appear to differ by about a factor of two at temperatures ( $T$ ) of  $\approx 400$  K. At this temperature, a statistically meaningful comparison is possible using the simulation times employed here (about 20 ps). Unfortunately, at lower temperatures such a quantitative comparison will require longer simulation times.

In addition to comparing BO and CP simulations, we have carried out a detailed analysis of the effect of proton quantum motion on computed structural and dynamical properties, by using the results of extended classical simulations with empirical inter-atomic forces. Our findings indicate that the inclusion of proton quantum effects would bring the DFT results obtained here in much better agreement with experiment, for both RDFs and

diffusion coefficients, and that their inclusion is crucial to accurately describe the properties of water at ambient conditions. In agreement with most previous studies, we find that proton quantum effects tend to give softer RDFs and faster diffusion than classical (Newtonian) simulations. We also find that the effect of proton quantum motion on calculated RDFs and diffusion coefficients at 300 K is the same as that obtained by increasing the ionic temperature by about 50 or 100 K at constant density, when using a rigid or flexible water model, respectively.

The rest of the paper is organized as follows. Section II contains a description of the methods used in both *ab initio* and classical MD simulations of water and Section III describes our results in detail. In particular, in Section IIIA we report a comparison between CP and BO simulations, and in Section IIIB we discuss possible sources of the apparent disagreement with experiment, namely the absence of proton quantum effects and the GGA functional (PBE) adopted here. The effect of temperature variations between 300 and 450 K on water at ambient density is analyzed in Section IIIC. Finally, Section IV contains our conclusions.

## II. METHODS

We have performed a series of molecular dynamics simulations<sup>11</sup> of liquid water with both *ab initio* and classical potentials. The *ab initio* molecular dynamics simulations are based on density functional theory with the PBE<sup>4</sup> generalized gradient approximation. Electron-ion interactions are treated with norm-conserving non-local pseudopotentials of the Hamann type<sup>12,13</sup>, and with the Kohn-Sham orbitals and charge density expanded in plane waves up to a kinetic energy cutoff of 85 and 340 Ry, respectively. In each simulation, the starting configuration was generated by performing 500 ps of classical molecular dynamics with the TIP5P potential<sup>14</sup>, followed by 3 ps of *ab initio* molecular dynamics with a weakly coupled velocity scaling thermostat set at the given target temperature. The thermostat was then removed and all reported statistics were collected under constant energy conditions.

For the Born-Oppenheimer (BO) simulations, the system consists of 64 water molecules in a cubic box of length 12.43 Å with periodic boundary conditions. At each molecular dynamics timestep, the wavefunction was relaxed to the ground state by preconditioned steepest descent with Anderson acceleration<sup>15</sup>. For a timestep of 0.24 fs, 12 electronic iterations were found to be sufficient to converge the total energy to within  $10^{-9}$  a.u. at each molecular dynamics iteration. Under these simulation conditions, the drift in the total energy was found to be equivalent to a 0.27 K/ps increase in the system temperature.

In the Car-Parrinello (CP) simulations, a slightly smaller system size of 54 water molecules in a cubic box of length 11.7416 Å was used. The electronic degrees of

TABLE I: Geometry and potential parameters defined as in Refs.<sup>14,16</sup> for the TIP5P water models.

	TIP5P	TIP5P (PM C)
$q_H$ (e)	0.241	0.251
$q_L$ (e)	-0.241	-0.251
$r_O$ (Å)	3.12	3.12
$\epsilon_O$ (kcal/mol)	0.16	0.16
$r_{OH}$ (Å)	0.9572	0.9572
$r_{OL}$ (Å)	0.70	0.70
$\angle HOH$ (deg)	104.52	104.52
$\angle LOL$ (deg)	109.47	109.47

freedom were propagated with a fictitious mass of  $m = 340$  a.u., and with a molecular dynamics timestep of 0.07 fs.

All classical simulations were performed with the Tinker simulation package<sup>17</sup> under constant volume and temperature conditions for systems of 64 rigid water molecules. A molecular dynamics timestep of 0.5 fs was used and the simulation temperature was maintained with a weakly coupled Berendsen-type thermostat<sup>18</sup>. Long-range electrostatic interactions were included with the particle-mesh Ewald method<sup>19</sup>. Both the TIP5P<sup>14</sup> and the TIP5P (PM C)<sup>16</sup> potentials, which are defined in Table I, have been examined.

## III. RESULTS

### A. Comparison of CP and BO dynamics at 300 K

In Ref.<sup>3</sup>, we have shown that in CP simulations of water at ambient conditions, one can vary the fictitious mass parameter,  $m$ , within a suitable range without significantly altering the results of the simulations. In particular, it was found that when  $m = 1=5$ , where  $M$  is the mass of the H or D atom in the simulation, the average structural properties and computed diffusion coefficients appear to be insensitive to the choice of  $m$ . This is in contrast to simulations performed with large values of  $m$  that lead to significant changes in both the structure and diffusion of the liquid. As discussed in Ref.<sup>3</sup>, the reason for the dramatic changes observed as  $m$  is increased from  $m = 1=5$  are due to a direct overlap of the fictitious electronic spectra with the highest frequency ionic spectra. In other words, as long as the fictitious electronic degrees of freedom can be adiabatically decoupled from the ionic degrees of freedom, the Car-Parrinello technique yields accurate results. However, as argued by Tangney et al.<sup>10</sup>, exact adiabatic separation in a Car-Parrinello simulation is never actually achieved, even for relatively small values of  $m$ . The reason for this is because in addition to the high frequency components in the ionic spectra that can lead to direct coupling to fictitious electronic degrees of freedom, there are additional  $m$ -dependent errors associated with the low-frequency components of the ionic motion. The impact of a particular choice of  $m$  can be

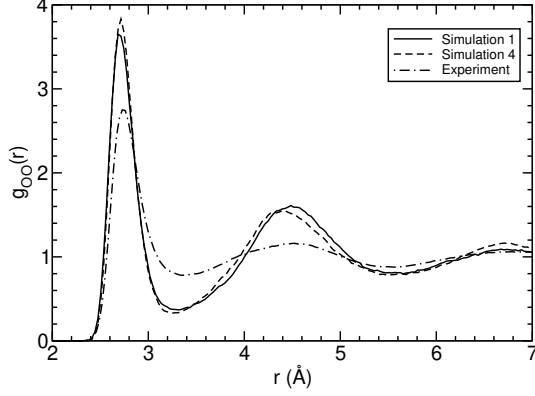


FIG. 1: Comparison of the oxygen-oxygen radial distribution functions obtained in BO and CP simulations at a temperature of 300 K. The solid line corresponds to CP dynamics, the dashed line to BO dynamics, and the dot-dashed line to experiment<sup>8</sup>.

assessed in a direct fashion by comparing Car-Parrinello simulations to so-called Born-Oppenheimer (BO) simulations of water, where the wavefunctions are converged to the ground state at each molecular dynamics time step.

In Figs. 1 to 3 the oxygen-oxygen, oxygen-hydrogen and hydrogen-hydrogen radial distribution functions (RDFs)<sup>20</sup> obtained with CP (Simulation 1) and BO (Simulation 4) *ab initio* MD at a temperature of approximately 300 K are shown along with the corresponding distribution functions obtained by experiment<sup>8</sup>. As can be seen, both the BO and CP simulations of water at 300 K lead to an overstructured liquid as compared to experiment. In addition, these results confirm the previous observation that, as long as  $\beta$  is chosen appropriately, CP simulations of water at ambient conditions can give a consistent description of the liquid RDFs<sup>3</sup>.

The large amount of overstructure seen in Figs. 1 to 3 appears in the simulation within a relatively short timescale ( $\sim 2$  ps), and can be readily observed, even when starting the simulation from a classical theoretical model or a higher simulation temperature, which may yield a less structured  $g(r)$ . This relatively short timescale should not be confused with the much longer timescale required to obtain statistically independent data points for a given RDF<sup>3</sup>, which will be discussed further in Section IIIB 3.

In addition to the average structural properties of the liquid, we have computed the diffusion coefficient using the Einstein relation:

$$6D = \lim_{t \rightarrow \infty} \frac{d}{dt} \langle \mathbf{r}_i(t) - \mathbf{r}_i(0) \rangle^2 : \quad (1)$$

To evaluate Eq. 1, the mean square displacement (MSD) of the oxygen atoms as a function of time was determined by averaging over the trajectories with multiple starting

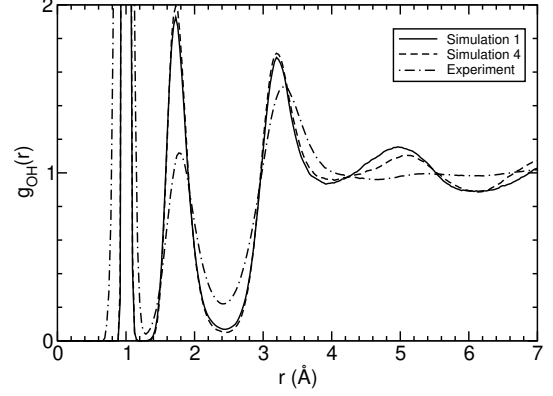


FIG. 2: Comparison of the oxygen-hydrogen radial distribution functions obtained in BO and CP simulations at a temperature of 300 K. The solid line corresponds to CP dynamics, the dashed line to BO dynamics, and the dot-dashed line to experiment<sup>8</sup>.

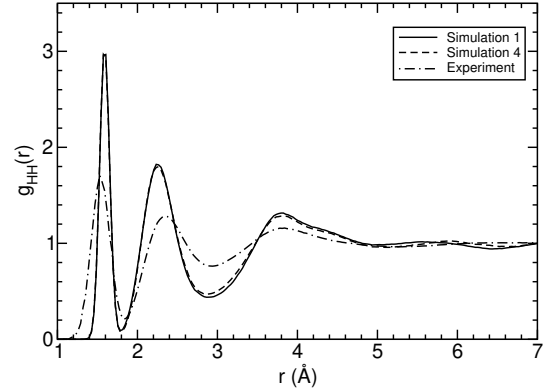


FIG. 3: Comparison of the hydrogen-hydrogen radial distribution functions obtained in BO and CP simulations at a temperature of 300 K. The solid line corresponds to CP dynamics, the dashed line to BO dynamics, and the dot-dashed line to experiment<sup>8</sup>.

configurations that are evenly spaced by 4 fs. The slope of the resulting MSD was determined in the range of 1 to 10 ps and used to compute the diffusion coefficient,  $D$ . As shown in Table II, the computed diffusion coefficients obtained in this manner for both the CP and BO simulations at 300 K are much smaller (by at least a factor of ten) than  $D$  measured experimentally at the same temperature<sup>21</sup>. Although the difference between the simulated and measured diffusion coefficients are statistically meaningful, the difference between the CP and BO diffusion coefficients at 300 K are not. Indeed, to make a quantitative comparison between diffusion coefficients that are in the range  $10^{-7}$  to  $10^{-6} \text{ cm}^2/\text{sec}$ , orders of

TABLE II: For each simulation performed in this work, the type of simulation (Car-Parrinello { CP or Born-Oppenheimer { BO, number of molecules  $N$ , total simulation time (ps), average temperature (K), diffusion coefficient  $D$  ( $\text{cm}^2/\text{s}$ ), position ( $\text{\AA}$ ) and value of  $r_{\text{st}}$  maximum and minimum in the  $g_{\text{O}}(r)^{20}$ , average temperature (K), and average coordination (CN) of the water molecules are listed. All simulations are for  $\text{H}_2\text{O}$  with the PBE density functional. CP simulations were carried out with a fictitious electron mass of 340 (1100) a.u. for flexible (rigid) water. The last row contains measured diffusion coefficients<sup>21</sup> and structural data<sup>8</sup> for water at ambient conditions.

Sim.	Type	N	Time	$T_{\text{avg}}$	$D$	$R[g(r)_{\text{max}}]$	$g(r)_{\text{max}}$	$R[g(r)_{\text{min}}]$	$g(r)_{\text{min}}$	CN
1	CP	54	19.8	296	$2.4 \times 10^{-6}$	2.69	3.65	3.32	0.37	4.2
2	CP	54	18.8	345	$5.0 \times 10^{-6}$	2.72	3.21	3.35	0.42	4.3
3	CP	54	22.0	399	$2.2 \times 10^{-5}$	2.75	2.60	3.41	0.73	4.6
4	BO	64	20.5	306	$7.9 \times 10^{-7}$	2.72	3.83	3.25	0.33	4.1
5	BO	64	20.7	349	$3.3 \times 10^{-6}$	2.72	3.49	3.30	0.40	4.2
6	BO	64	18.6	393	$1.2 \times 10^{-5}$	2.73	3.10	3.40	0.56	4.6
7	BO	64	10.5	442	$3.9 \times 10^{-5}$	2.75	2.63	3.44	0.74	4.8
8	CP-Rigid	54	24.5	315	$1.3 \times 10^{-5}$	2.75	2.92	3.41	0.61	4.6
9	CP-Rigid	54	26.3	345	$3.3 \times 10^{-5}$	2.75	2.61	3.41	0.77	4.7
10	TIP5P (PIMC), $P=1$	64	500.0	300	$2.6 \times 10^{-6}$	2.69	3.61	3.29	0.43	4.1
11	TIP5P (PIMC), $P=1$	64	500.0	350	$2.8 \times 10^{-5}$	2.72	2.84	3.38	0.78	4.6
12	TIP5P (PIMC), $P=5$	216		300		2.73	2.76	3.44	0.77	
	Experiment			298	$2.3 \times 10^{-5}$	2.73	2.75	3.36	0.78	4.7

magnitude longer simulation times than those used here would be required.

## B. Comparison of ab-initio MD to experiment and analysis of discrepancies

There are a number of possible explanations for the observed overstructure and slow diffusion of our DFT/GGA-based molecular dynamics simulations of water. In the following, we concentrate on three of the most likely causes. The first is related to possible inaccuracies of the PBE functional in describing hydrogen bonding. The second is related to the neglect of proton quantum effects. The third is related to the timescales used in the ab initio simulations.

### 1. Accuracy of DFT/GGA for the water monomer and dimer

In order to better quantify the accuracy of the DFT/GGA functional used here, it is useful to re-examine the computed properties of the water monomer and dimer (for the interested reader, a more comprehensive review of the water monomer and dimer properties as computed within DFT was recently published in Ref.<sup>22</sup>).

As shown in Table III, we have examined the use of a number of DFT exchange-correlation functionals, including LDA<sup>30,31</sup>, GGA (PBE<sup>4</sup> and BLYP<sup>5,6</sup>), and hybrid (PBE1PBE<sup>32</sup> and B3LYP<sup>33</sup>) functionals. Also included in Table III are the results of several CCSD(T) calculations<sup>23,24</sup> as well as the relevant experimental measurements<sup>25,26,27,28,29</sup>. The CCSD(T) results represent the most accurate quantum chemistry computations of the water monomer and dimer to date. For all of the

TABLE III: Selected properties of the water monomer and dimer. All reported distances are in  $\text{\AA}$ . DM refers to the dipole moment in Debye,  $\epsilon_{\text{iso}}$  is the isotropic polarizability in  $\text{\AA}^3$ ,  $\angle \text{H O H}$  is the intermolecular hydrogen bond angle, and  $D_e$  is the binding energy of the water dimer in kcal/mol.

Method	Monomer				Dimer		
	$r_{\text{OH}}$	$\angle \text{H O H}$	DM	$\epsilon_{\text{iso}}$	$r_{\text{OO}}$	$\angle \text{O H O}$	$D_e$
LDA	0.970	104.9	1.87	1.52	2.71	172.8	9.02
PBE	0.970	104.2	1.81	1.55	2.90	173.7	5.10
BLYP	0.972	104.5	1.80	1.54	2.95	171.6	4.18
PBE1PBE	0.959	104.9	1.85	1.42	2.90	174.1	4.90
B3LYP	0.962	105.1	1.85	1.45	2.92	172.1	4.57
CCSD(T)	0.959 <sup>a</sup>	104.2 <sup>a</sup>			2.91 <sup>b</sup>	174.5 <sup>b</sup>	5.02 <sup>b</sup>
Exp.	0.957 <sup>c</sup>	104.5 <sup>c</sup>	1.85 <sup>d</sup>	1.43 <sup>e</sup>	2.98 <sup>f</sup>	174.0 <sup>f</sup>	5.44 <sup>g</sup>

<sup>a</sup>Ref.<sup>23</sup>, <sup>b</sup>Ref.<sup>24</sup>, <sup>c</sup>Ref.<sup>25</sup>, <sup>d</sup>Ref.<sup>26</sup>, <sup>e</sup>Ref.<sup>27</sup>, <sup>f</sup>Ref.<sup>28</sup>, <sup>g</sup>Ref.<sup>29</sup>.

DFT-based calculations reported in Table III we have used the electronic structure program Gaussian 03<sup>34</sup> with the aug-cc-pVTZ basis set<sup>35</sup>.

For the computed bond distances and angles, the majority of the tested functionals perform reasonably well. The most notable exception is the oxygen-oxygen distance in the LDA water dimer calculation, which is much too short. Although the computed dipole moments of the water monomer are also in good agreement with each other, it is interesting to note that the isotropic polarizabilities are systematically too large at the LDA and GGA level of theory. This is due to the well-known tendency of local DFT functionals to underestimate the HOMO-LUMO gap of molecular systems, which in turn

leads to an overestimation of the molecular polarizability. A more accurate, hybrid functionals are considered, this general tendency seems to disappear. In Table III we also show computed binding energies. As expected, the LDA binding energy is much too large. The remainder of the DFT functional binding energies are in relatively good agreement with each other, as well as with the CCSD(T) calculation and the experimental measurement.

Given the differences in the water dimer binding energies found with BLYP and PBE (the BLYP binding energy is 1 kcal/mol smaller than PBE), one might think that the PBE functional would give more structured RDFs and slower diffusion of the liquid, as compared to BLYP. In our previous work we could not resolve any statistically significant difference between PBE and BLYP results. However, comparison of the present CP results with those of Chen et al.<sup>36</sup> (which were obtained with a sufficiently small cuttious mass ( $= 400$  a.u.) and the BLYP functional) seem to show differences which would be consistent with the idea that BLYP yields less structured RDFs than PBE. At this point, it is difficult to draw any firm conclusions, as the time scale of both the present work and the simulations of Ref.<sup>36</sup> are probably too small to statistically resolve differences.

We note that there is a very good agreement between the PBE and the CCSD(T) binding energies, and overall the water monomer and dimer properties listed in Table III appear to be well reproduced by the PBE functional. Although these zero temperature, gas phase results do not necessarily insure an equally good performance of the functional in the liquid state, they are very promising. We also note that the PBE functional appears to be quite accurate in reproducing the sublimation energy, lattice constant and bulk modulus of ice-Ih<sup>37</sup>. It would be interesting to explore the accuracy of other functionals, along the lines proposed in Ref.<sup>2,38</sup>, especially of hybrid functionals, but this falls beyond the scope of the present investigation.

## 2. Proton quantum effects

In addition to possible inaccuracies in the DFT/PBE treatment of water, it is plausible that some amount of the observed overstructure is due to the neglect of the quantum motion of the hydrogen atoms. As pointed out in Ref.<sup>39</sup>, at 300 K,  $k_B T \approx 200$  cm<sup>-1</sup>, whereas the high frequency intramolecular modes in water range from 1000 to 3500 cm<sup>-1</sup>. Therefore, in the real quantum system, the amount of thermal energy available to excite vibrational modes is much smaller than the lowest possible intramolecular vibrational excitations,

$$h\nu \gg k_B T: \quad (2)$$

In other words, the quantum system will be restricted to its vibrational ground state at a temperature of 300 K, and the quantum and the classical system will be qualitatively different in terms of the distribution of vibra-

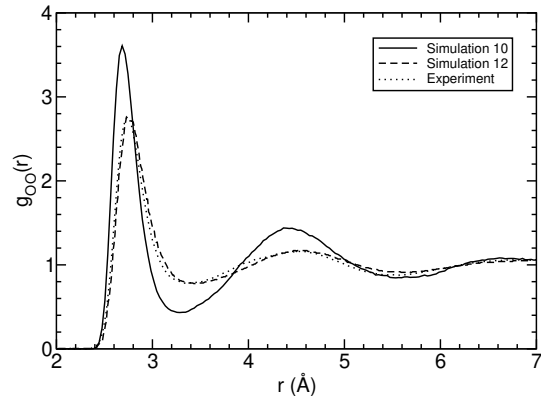


FIG. 4: The oxygen-oxygen radial distribution function obtained in TIP5P (PIMC) simulations (see text) of water at a density of 0.997 g/cc, and a temperature of 300 K. The solid line corresponds to a simulation performed with  $P=1$  (no path integral sampling), the dashed line to  $P=5$  (taken from Ref.<sup>16</sup>), and the dotted line to experiment<sup>8</sup>.

tional energy. When using empirical potentials with intramolecular flexibility, quantum effects can, to some extent, be implicitly included in the potential parameterization. However, in the case of ab initio based methods, the possibility of implicitly accounting for quantum effects by renormalizing the interaction potential is, by definition, not an option.

In principle, the effect of the proton quantum motion can be accounted for with path-integral (PI) methods<sup>40</sup>. To date, combining PI sampling of ionic trajectories with empirical interaction potentials has been found to lead to an overall softening of the RDFs of water at ambient conditions<sup>16,41,42,43,44</sup>. However, the majority of these simulations have been performed with empirical potentials that already include some amount of quantum effects. In particular, it is common to use classical molecular dynamics or Monte Carlo sampling in the parameterization of an interatomic potential, with the goal of fitting experimental data as well as possible. Within this procedure, agreement with experiment is achieved by renormalizing interatomic interactions so as to include proton quantum effects, which are not explicitly treated by classical molecular dynamics or Monte Carlo. There are, however, important exceptions to this general procedure. In particular, in Ref.<sup>16</sup>, the TIP5P potential was reparameterized with PIMonte Carlo sampling instead of classical Monte Carlo sampling. The resulting potential, which we will refer to here as TIP5P (PIMC), is nearly identical to the original TIP5P potential except for the magnitude of the charges on the hydrogen and lone-pair sites, which have been slightly increased (see Table I). The TIP5P (PIMC) potential opens up the interesting possibility of directly examining, in the context of a rigid water model, the extent to which quan-

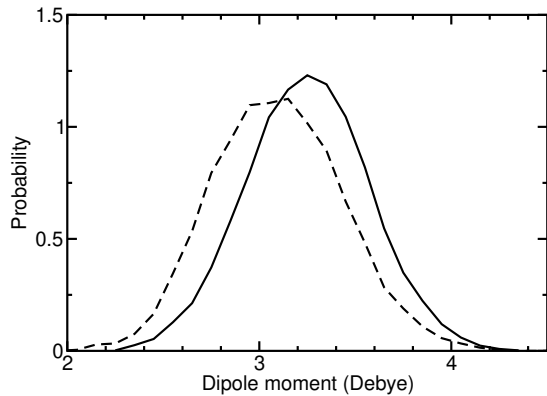


FIG. 5: The probability distribution of water molecule dipole moments obtained in CP simulations of water at a temperature of 300 K. The solid line corresponds to a simulation performed with the fictitious mass = 340 au, and the dashed line to a simulation with = 760 au.

tum effects can soften the RDF of water. As shown in Fig. 4, when the TIP5P (PIMC) potential is used in a classical molecular dynamics simulation with  $P=1$  ( $P$  refers to the number of beads used to represent the path integrals), the resulting oxygen-oxygen RDF becomes severely overstructured as compared to a PIMonte Carlo calculation with the TIP5P (PIMC) potential where  $P=5$  is used (taken from Ref.<sup>16</sup>). The amount of overstructure seen in Fig. 4 is nearly identical to the BO and CP RDFs presented earlier in Fig. 1. In addition, in the TIP5P (PIMC),  $P=1$  simulation the diffusion coefficient of the liquid is  $2.2 \times 10^{-6} \text{ cm}^2/\text{s}$ , which is approximately ten times smaller than the experimental value; this value is also in qualitative agreement with the corresponding BO and CP simulations performed at 300 K (see Table II). These results indicate that including proton quantum effects may bring the ab initio results presented here into significantly better agreement with experiment and that neglect of these effects is probably responsible for the majority of the discrepancy between experiment and DFT results.

Along with the existing PI studies based on empirical water potentials<sup>16,41,42,43,44</sup>, Chen, et al.<sup>45</sup> recently demonstrated the feasibility of directly performing PI sampling and CP simulations of water. However, instead of the expected softening of the liquid structure, Chen, et al.<sup>45</sup> found the rather surprising result that quantum effects may actually increase the structure of water. The reason for this increase was attributed to an enhancement of the individual water molecule's dipole moments when proton quantum effects are included in the calculations. In particular, an analysis based on maximally localized Wannier functions<sup>46</sup> was used to demonstrate that the average dipole moment of water molecules increases from 3.08 Debye in their CP simulation performed with clas-

sical ion dynamics to an average value of 3.19 Debye when PI sampling is included. Although we have used a different GGA functional (PBE instead of the BLYP functional used in Ref.<sup>45</sup>), it is interesting to note that in our CP simulations we find a dipole moment of 3.24 Debye when a fictitious mass of = 320 au is used (a value of = 500 au was reported in Ref.<sup>45</sup>). As shown in Fig. 5, when a larger value of the fictitious mass is used (= 740 au) the average dipole moment decreases to 3.06 Debye. An average value of 3.24 Debye found here is not consistent with the results reported in Ref.<sup>45</sup>, and opens up the possibility that the role of quantum effects in path integral/DFT-based simulations of water may not be completely understood. Indeed, simulations using PI sampling with a flexible water model are known to be quite difficult to converge<sup>16</sup>. In this regard, additional investigations, which are beyond the scope of this work, are most likely needed where the convergence of the various technical parameters involved in PI simulations are examined in detail.

### 3. Timescales

As discussed in Ref.<sup>3</sup>, another approximation that needs to be considered is the length of the time interval over which averages, such as the RDFs, are taken. In the case of ab initio molecular dynamics simulations, which are usually limited to relatively short timescales (10 to 20 ps), this can be a particularly significant effect. In this regard, it is important to determine the time interval outside which neighboring simulation data points are no longer correlated, and thus statistically significant. In Ref.<sup>3</sup> a method based on a combination of re-blocking and autocorrelation function techniques was used for determining this time interval along with an estimate of the variance for individual bins of a RDF. Because this method requires simulation trajectories of at least 1 to 2 orders of magnitude longer than the actual correlation time, a 2 ns classical MD simulation of 32 TIP5P water molecules under ambient conditions was used for the analysis. Based on this trajectory, correlation times as long as 10 ps were observed for the oxygen-oxygen RDF. However, we note that the diffusion coefficient for 32 TIP5P water molecules under ambient conditions is  $2.1 \times 10^{-5} \text{ cm}^2/\text{s}$ , which is at least 10 times larger than what is found in our ab initio BO and CP simulations at 300 K. Therefore, in order to have an estimate of the RDF correlation time and variance relevant to our 300 K BO and CP simulations, it is more appropriate to use the TIP5P (PIMC),  $P=1$  potential for this analysis. In Fig. 6, the computed correlation time for the oxygen-oxygen RDF bins is shown for both TIP5P and the TIP5P (PIMC),  $P=1$  simulations of ambient water. As can be seen near the regions of the first peak in  $g_{\text{OO}}(r)$ , the correlation times increase from 10 ps with the TIP5P potential to 20 ps for the TIP5P (PIMC) potential. Although there is a considerable amount of

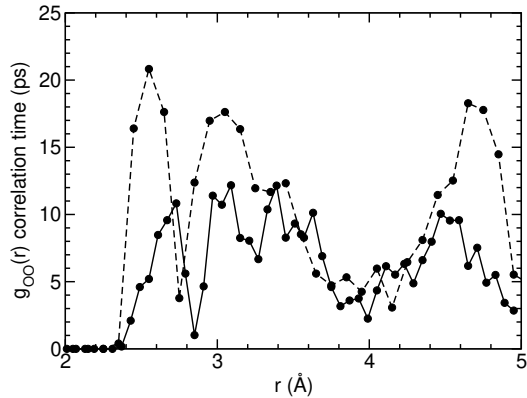


FIG. 6: The oxygen-oxygen RDF correlation times computed from classical molecular dynamics simulations using the TIP5P (solid line) and TIP5P (PIMC),  $P=1$  (dashed line) potentials at ambient conditions. The points correspond to the correlation time for each bin that was used to collect the distribution function.

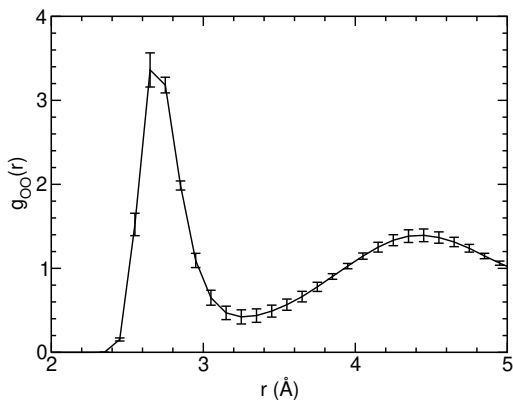


FIG. 7: Oxygen-oxygen RDF for the TIP5P (PIMC),  $P=1$  classical potential. The error bars correspond to the square root of the variance.

scatter in the correlation times shown in Fig. 6, this analysis does provide a useful lower bound to the expected correlation times of the radial distribution function bins.

In Fig. 7, an estimate of the variance in the oxygen-oxygen RDF bins is shown for a block of length equal to the TIP5P (PIMC) correlation times displayed in Fig. 6. As discussed in Ref.<sup>3</sup>, the error bars shown in Fig. 7 are representative of the uncertainties that should be expected when comparing independent 20 ps simulations of water that are characterized by a diffusion coefficient on the order of  $10^{-6} \text{ cm}^2/\text{s}$ .

In addition to uncertainties in structural properties, the limited timescales of a typical first-principles simulation of water can strongly influence dynamical properties

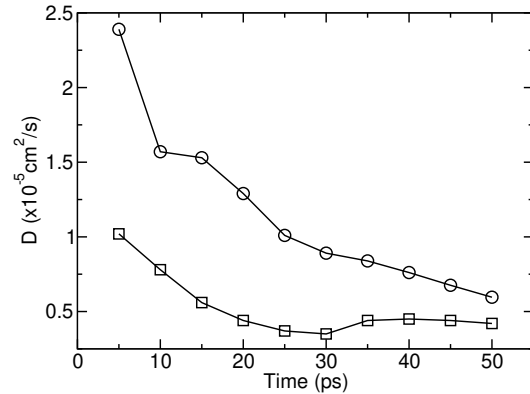


FIG. 8: The computed diffusion coefficient as a function of simulation time for the TIP5P (PIMC),  $P=1$  potential at a temperature of 300 K and a density of 0.997 g/cc. The circles correspond to a simulation that was initially equilibrated with the TIP5P potential at 600 K and the squares to a simulation that was equilibrated with the TIP5P potential at 300 K (see text for details).

such as computed diffusion coefficients. In order to illustrate this effect we have performed two simulations of 64 water molecules with the TIP5P (PIMC),  $P=1$  potential that differ in how the starting configurations were equilibrated. In the first simulation, the initial starting configuration was taken from a 500 ps TIP5P simulation at a temperature of 300 K. The simulation was then continued for an additional 53 ps with the TIP5P (PIMC),  $P=1$  potential at a temperature of 300 K. This simulation closely resembles the equilibration procedure that was used for the first-principles simulations presented here. In the second simulation, the initial starting configuration was taken from a 500 ps TIP5P simulation at a temperature of 600 K. The simulation was then continued, as before, for an additional 53 ps with the TIP5P (PIMC),  $P=1$  potential at a temperature of 300 K. The last 50 ps (the first 3 ps were discarded) of these two simulations were analyzed by computing the diffusion coefficient via Eq. 1 as a function of the simulation time at 5 ps intervals. As can be seen in Fig. 8, the specifics of the initial equilibration phase on the diffusion coefficients can be rather dramatic. In particular, an equilibration phase that involves annealing at a higher temperature can lead to a significant overestimation of the diffusion coefficient with respect to the infinite time limit, even for simulations as long as 50 ps.

### C. The effect of temperature in simulations of water

As pointed out in Ref.<sup>41</sup> for the ST2 water model, and in Ref.<sup>42</sup> for the SPC and TIP4P models, the main struc-

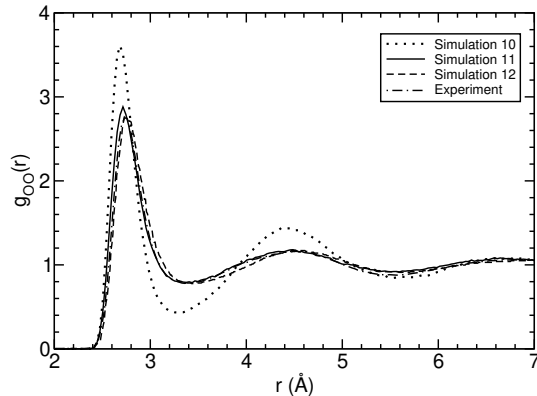


FIG. 9: The oxygen-oxygen radial distribution function obtained in different TIP5P (PIMC) simulations. The dotted line corresponds to a simulation performed at 300 K with  $P=1$ , the solid line to 350 K with  $P=1$ , the dashed line to 300 K with  $P=5$  (taken from Ref.<sup>16</sup>), and the dashed-dotted line to experiment<sup>8</sup>.

tural changes that occur when going from a classical to a quantum description of water at 300 K are similar to simply increasing the temperature of the classical simulation by 50 K. In order to examine if similar results are obtained when the TIP5P (PIMC) potential is used, we have performed classical simulations ( $P=1$ ) of water with the TIP5P (PIMC) potential at temperatures of 300 and 350 K (simulations 10 and 11 in Table II). In Fig. 9, the oxygen-oxygen RDF obtained in these simulations are compared to TIP5P (PIMC),  $P=5$  at 300 K<sup>16</sup>, and to experiment at 300 K<sup>8</sup>. As expected from previous investigations<sup>41,42</sup>, the main structural differences between the classical and quantum fluid described by the TIP5P (PIMC) are remarkably similar to a 50 K temperature increase in the classical simulation temperature at constant density. In addition to the observed structural changes, the 50 K temperature increase also causes the diffusion coefficient of classical TIP5P (PIMC) water to increase from  $2.2 \cdot 10^{-6} \text{ cm}^2/\text{s}$  to  $3.0 \cdot 10^{-5} \text{ cm}^2/\text{s}$ , which is in much better agreement with the experimental measurement of  $2.2 \cdot 10^{-5} \text{ cm}^2/\text{s}$  for water under ambient conditions<sup>21</sup>. We also note that approximately accounting for quantum effects via temperature scaling is a technique that has been used in a variety of materials other than water<sup>47,48</sup>.

Given the agreement of results obtained with the TIP5P (PIMC) potential when including quantum effects, and increasing the classical simulation temperature, it is interesting to examine if a similar decrease in structure occurs in DFT simulations of water as a function of temperature. However, it is important to note that the TIP5P (PIMC) potential used above is based on a rigid water model that does not allow for intermolecular flexibility. Therefore, to make a direct comparison be-

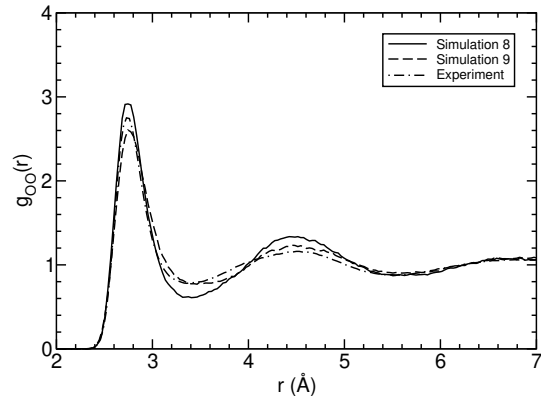


FIG. 10: The oxygen-oxygen radial distribution function obtained in CP simulations of rigid water. The solid line corresponds to a simulation performed at 315 K, the dashed line to a simulation at 345 K, and the dashed-dotted line to experiment<sup>8</sup>.

tween classical and *ab initio* MD, we have first examined the effects of increasing the temperature in CP simulations of rigid water. Our results are reported in Fig. 10. The technical details of the simulations are the same as those used in simulation B of Ref.<sup>49</sup>. As can be seen by comparing Figs. 1 and 10, although the amount of structure in the CP rigid water simulation at a temperature of 315 K (simulation 8) is smaller than the one observed in the flexible water simulation (simulation 1 at 296 K), there is still a noticeable amount of overstructure as compared to experiment. Also shown in Fig. 10 are the results of a CP simulation of rigid water at a temperature of 345 K (simulation 9). As was seen in the case of the TIP5P (PIMC) potential, at a temperature of 350 K the oxygen-oxygen radial distribution function is in good agreement with the corresponding experimental measurement at 300 K. Therefore, we expect that an increase in temperature has a similar effect on the liquid structure with both the TIP5P (PIMC) potential and DFT/rigid water. This provides indirect evidence that RDFs computed with TIP5P (PIMC) and DFT/rigid water will soften to the same extent when PI sampling is performed.

In addition to CP simulations of rigid water, we have also investigated the effect of temperature in CP and BO simulations of flexible water at constant density. As shown in Figs. 11 to 13 for CP dynamics, and in Figs. 14 to 16 for BO dynamics, an increase in the simulation temperature decreases the overstructure in the radial distribution functions found in the corresponding simulations at 300 K. However, close inspection of Figs. 11 to 16 reveals that both CP and BO simulations of flexible water require a significantly larger temperature increase than the simulations of rigid water in order to bring the radial distribution functions into agreement with experiment at



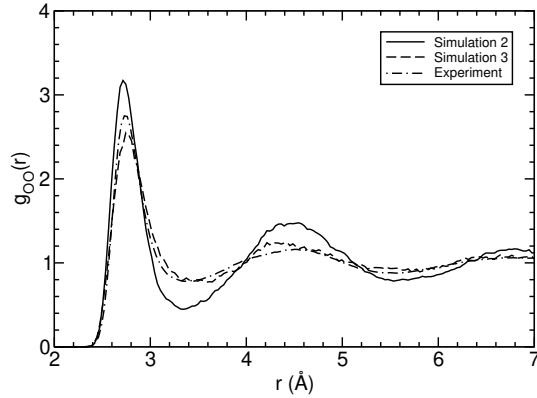


FIG. 11: The oxygen-oxygen radial distribution function obtained in CP simulations of water at different temperatures. The solid line corresponds to a simulation performed at 350 K, the dashed line to 400 K, and the dashed-dotted line to experiment<sup>8</sup>.

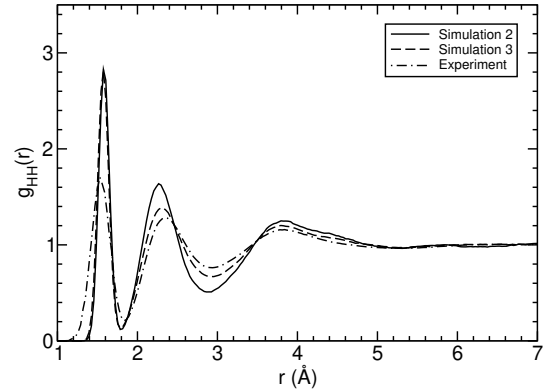


FIG. 13: The hydrogen-hydrogen radial distribution function obtained in CP simulations of water at different temperatures. The solid line corresponds to a simulation performed at 350 K, the dashed line to 400 K, and the dashed-dotted line to experiment<sup>8</sup>.

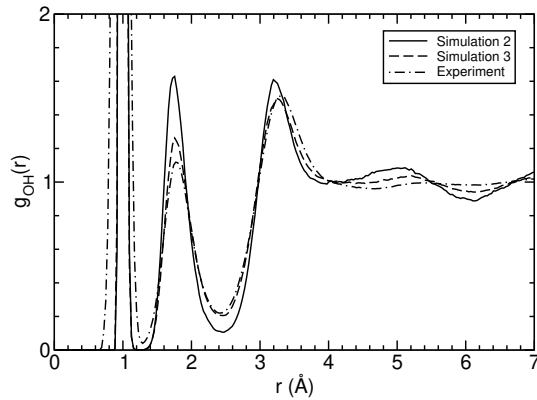


FIG. 12: The oxygen-hydrogen radial distribution function obtained in CP simulations of water at different temperatures. The solid line corresponds to a simulation performed at 350 K, the dashed line to 400 K, and the dashed-dotted line to experiment<sup>8</sup>.

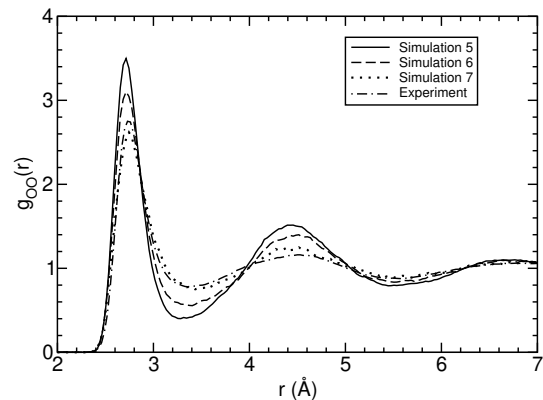


FIG. 14: The oxygen-oxygen radial distribution function obtained in BO simulations of water at different temperatures. The solid line corresponds to a simulation performed at 350 K, the dashed line to 400 K, the dotted line to 450 K, and the dashed-dotted line to experiment<sup>8</sup>.

300 K.

In Fig. 17 the computed diffusion coefficients for different simulations are shown as a function of the simulation temperature. Also shown in Fig. 17 are the experimentally measured diffusion coefficients of water as a function of temperature<sup>21,50</sup>. Consistent with the oxygen-oxygen radial distribution functions shown in Fig. 10, the temperature dependence of the CP rigid water diffusion coefficient is similar to that of TIP5P (PIMC),  $P=1$ . This indicates that at approximately 350 K the simulation diffusion coefficient obtained with CP-rigid water simulations is equal to the experimental value at 300 K.

In the flexible water simulations, the temperature de-

pendence of the diffusion coefficients are quite different. Over the same temperature range of 300 to 350 K, the computed diffusion coefficients increase at a much slower rate than in the rigid water simulations, and temperatures of 400 K in the CP simulation and 415 K in the BO simulations are needed in order to obtain diffusion coefficients comparable to experiment at 300 K. These findings are in qualitative agreement with previous observations based on empirical potentials, which found that the use of a rigid water approximation tends to lead to an overall decrease in structure of the liquid and faster diffusion as compared to a flexible representation with the same intramolecular potential<sup>13</sup>.

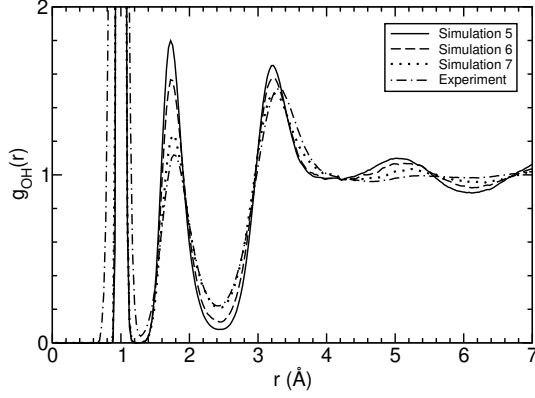


FIG. 15: The oxygen-hydrogen radial distribution function obtained in BO simulations of water at different temperatures. The solid line corresponds to a simulation performed at 350 K, the dashed line to 400 K, the dotted line to 450 K, and the dashed-dotted line to experiment<sup>8</sup>.

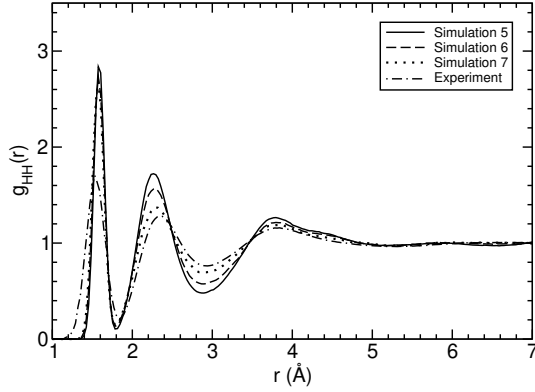


FIG. 16: The hydrogen-hydrogen radial distribution function obtained in BO simulations of water at different temperatures. The solid line corresponds to a simulation performed at 350 K, the dashed line to 400 K, the dotted line to 450 K, and the dashed-dotted line to experiment<sup>8</sup>.

We note that for all of the temperatures considered here, the diffusion coefficients obtained with CP dynamics (with  $m = 340$  a.u.) appear to be approximately two times larger than in the corresponding BO simulations. As mentioned earlier in Section III A and discussed in more detail by Tangney et al.<sup>10</sup>, this difference between the computed diffusion coefficients in CP and BO simulations is most likely due to a small, but still significant, effect of the chosen fictitious mass value in the CP simulations.

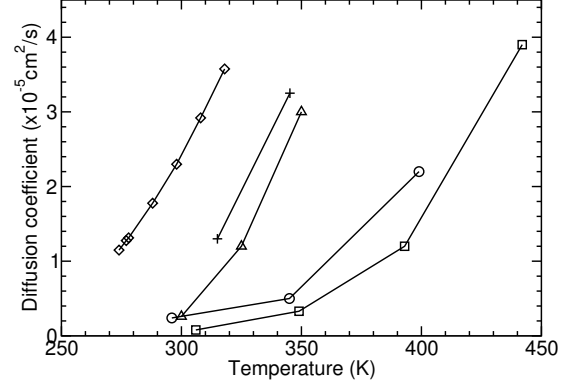


FIG. 17: The diffusion coefficient of water as a function of temperature. The diamonds correspond to the experimental measurements reported in Ref.<sup>21</sup>, crosses to rigid water CP, triangles to TIP5P (PM C),  $P = 1$ , circles to flexible water CP, and squares to flexible water BO. The lines are simply a guide to the eye.

#### IV. CONCLUSION

We have presented a series of 20 ps *ab initio* MD simulations of water at ambient conditions and temperatures ranging from 300 to 450 K, carried out using both the CP and BO techniques. Radial distribution functions obtained with both approaches are in excellent agreement with each other, provided an appropriately small fictitious mass is used in CP simulations. Differences have been observed in computed diffusion coefficients, those obtained with BO dynamics being systematically 2 times smaller than the corresponding CP values. However, these differences are statistically significant only at  $T \geq 400$  K, given the time span of our simulations (20 ps). These results indicate that even for relatively small values of the fictitious electronic mass, some coupling between the classical motion of electronic and ionic degrees of freedom is unavoidable in CP simulations, as pointed out by Tangney et al.<sup>10</sup>. Furthermore, the inaccuracies introduced by this coupling appear not to have a significant, quantitative effect on calculated structural properties; rather, their effect may be seen on dynamical properties such as the diffusion coefficient.

We have also presented an analysis of the effects of the proton quantum motion on computed structural and dynamical properties of water. Our results, obtained with a series of classical MD and PI calculations with empirical force fields, provide strong indications that the neglect of quantum effects may account for most of the discrepancy observed here between DFT-based simulations and experiment. We have found that including proton quantum effects is approximately equivalent to a temperature increase of 50 and 100 K, when using a rigid or a flexible water model, respectively, under constant volume

conditions. This is true for both RDFs and diffusion coefficients. We note that although quantum effects most certainly do have an influence on the properties of water at ambient conditions, the exact magnitude of this effect is still unclear. For example, all of the simulations shown here have been performed under constant volume conditions that corresponds to a density of  $0.997\text{g/cc}$ . It is likely that this does not correspond to the exact equilibrium density of water as described by the PBE functional, which may in turn have an effect on the precise temperatures needed to bring the RDFs and diffusion coefficients into agreement with experiment.

Finally, we note that inaccuracies in the DFT description of hydrogen bonding may be attributed to the choice of the local energy functional (PBE in this paper); the

use of hybrid functionals that provide a better agreement between measured and calculated gas phase polarizabilities may improve the description of the fluid as well.

## V. ACKNOWLEDGMENTS

We thank L.R. Pratt, D. Asthagiri and D. Prendergast for many useful discussions, and E.W. Draeger for performing the variance calculations used here. This work was performed under the auspices of the U.S. Dept. of Energy at the University of California/Lawrence Livermore National Laboratory under contract no. W-7405-Eng-48.

- <sup>1</sup> S. Izvekov and G.A. Voth, *J. Chem. Phys.* 116, 10372 (2002).
- <sup>2</sup> D. Asthagiri, L.R. Pratt, and J.D. Kress, *Phys. Rev. E* 68, 041505 (2003).
- <sup>3</sup> J.C. Grossman et al., *J. Chem. Phys.* 120, 300 (2004).
- <sup>4</sup> J.P. Perdew, K. Burke, and M. Ernzerhof, *Phys. Rev. Lett.* 77, 3865 (1996).
- <sup>5</sup> A.D. Becke, *Phys. Rev. A* 38, 3098 (1988).
- <sup>6</sup> C. Lee, W. Yang, and R.G. Parr, *Phys. Rev. B* 37, 785 (1988).
- <sup>7</sup> R. Car and M. Parrinello, *Phys. Rev. Lett.* 55, 2471 (1985).
- <sup>8</sup> A.K. Soper, *Chem. Phys.* 258, 121 (2000).
- <sup>9</sup> J.M. Sorenson, G. Huira, R.M. Glaeser, and T. Head-Gordon, *J. Chem. Phys.* 113, 9149 (2000).
- <sup>10</sup> P. Tangney and S. Scandolo, *J. Chem. Phys.* 116, 14 (2002).
- <sup>11</sup> F. Gygi, Qbox 1.15.0: A general ab initio molecular dynamics program, Lawrence Livermore National Laboratory, 2004.
- <sup>12</sup> D.R. Hamann, *Phys. Rev. B* 40, 2980 (1989).
- <sup>13</sup> L. Kleinman and D.M. Bylander, *Phys. Rev. Lett.* 48, 1425 (1982).
- <sup>14</sup> M.W. Mahoney and W.L. Jorgensen, *J. Chem. Phys.* 112, 8910 (2000).
- <sup>15</sup> D. Anderson, *J. Ass. Comput. Mach.* 12, 547 (1975).
- <sup>16</sup> M.W. Mahoney and W.L. Jorgensen, *J. Chem. Phys.* 115, 10758 (2001).
- <sup>17</sup> P. Ren and J.W. Ponder, *J. Phys. Chem. B* 107, 5933 (2003).
- <sup>18</sup> H.J.C. Berendsen et al., *J. Chem. Phys.* 81, 3684 (1984).
- <sup>19</sup> T. Darden, D. York, and L. Pedersen, *J. Chem. Phys.* 98, 10089 (1993).
- <sup>20</sup> All radial distribution functions computed between identical atom types have been normalized by  $\frac{4\pi}{N(N-1)}$  where  $V$  is the volume of the simulation cell and  $N$  is the number of atoms involved in the distribution function.
- <sup>21</sup> R.M. Mills, *J. Phys. Chem.* 77, 685 (1973).
- <sup>22</sup> X. Xu and I.W.A. Goddard, *J. Phys. Chem. A* 108, 2305 (2004).
- <sup>23</sup> G.S. Tschumper et al., *J. Chem. Phys.* 116, 690 (2002).
- <sup>24</sup> W. Kloppe, J.G.C.M. van Duinveeldt-van der Rijt, and F.B. van Duinveeldt, *Phys. Chem. Chem. Phys.* 2, 2227 (2000).
- <sup>25</sup> W.S. Benedict, N. Gailar, and E.K. Plyler, *J. Chem. Phys.* 24, 1139 (1975).
- <sup>26</sup> S.A. Clough, Y. Beers, G.P. Klein, and L.S. Rothman, *J. Chem. Phys.* 59, 2254 (1973).
- <sup>27</sup> W.F. Murphy, *J. Chem. Phys.* 67, 5877 (1977).
- <sup>28</sup> J.A. Odutola and T.R. Dyke, *J. Chem. Phys.* 72, 5062 (1980).
- <sup>29</sup> L.A. Curtiss, D.J. Frurip, and M. Blander, *J. Chem. Phys.* 71, 2703 (1979).
- <sup>30</sup> J.C. Slater, *Phys. Rev.* 81, 385 (1951).
- <sup>31</sup> S.H. Vosko, L. Wilk, and M. Nusair, *Can. J. Phys.* 58, 1200 (1988).
- <sup>32</sup> M. Ernzerhof and G.E. Scuseria, *J. Chem. Phys.* 110, 5029 (1999).
- <sup>33</sup> A.D. Becke, *J. Chem. Phys.* 98, 5648 (1993).
- <sup>34</sup> M.J. Frisch et al., Gaussian 03, Revision B.05, Gaussian, Inc., Pittsburgh PA, 2003.
- <sup>35</sup> R.A. Kendall, T.H. Dunning, and R.J. Harrison, *J. Chem. Phys.* 96, 6796 (1992).
- <sup>36</sup> B. Chen, I.I. Iam and J.M. Park, M. Parrinello, and M.L. Klein, *J. Phys. Chem. B* 106, 12006 (2002).
- <sup>37</sup> D.R. Hamann, *Phys. Rev. B* 55, 10157 (1997).
- <sup>38</sup> Y. Zang and W. Yang, *Phys. Rev. Lett.* 80, 890 (1998).
- <sup>39</sup> I.G. Tironi, R.M. Brunne, and W.F. van Gunsteren, *Chem. Phys. Lett.* 250, 19 (1996).
- <sup>40</sup> R.P. Feynman and A.R. Hibbs, *Quantum Mechanics and Path Integrals* (McGraw Hill, New York, 1965).
- <sup>41</sup> R.A. Kuharski and P.J. Rossky, *J. Chem. Phys.* 82, 5164 (1985).
- <sup>42</sup> G.S.D. Buono, P.J. Rossky, and J. Schnitker, *J. Chem. Phys.* 95, 3728 (1991).
- <sup>43</sup> J. Lobaugh and G.A. Voth, *J. Chem. Phys.* 106, 2400 (1997).
- <sup>44</sup> H.A. Stern and B.J. Berne, *J. Chem. Phys.* 115, 7622 (2001).
- <sup>45</sup> B. Chen, I. Ivanov, M.L. Klein, and M. Parrinello, *Phys. Rev. Lett.* 91, 215503 (2003).
- <sup>46</sup> P.L. Silvestrelli and M. Parrinello, *Phys. Rev. Lett.* 82, 3308 (1999).
- <sup>47</sup> C.Z. Wang, C.T. Chan, and K.M. Ho, *Phys. Rev. B* 42, 11276 (1990).
- <sup>48</sup> L.J. Porter, J. Li, and S.Y. Ip, *J. Nuc. Mat.* 246, 53 (1997).
- <sup>49</sup> M. Alesch, E. Schwegler, F. Gygi, and G. Galli, *J. Chem.*

Phys. 120, 5192 (2004).

<sup>50</sup> K. Krynicky, C. D. Green, and D. W. Sawyer, Faraday

Disc. Chem. Soc. 66, 199 (1978).